

## **Effect of Crystallization Temperature on the Synthesis of SAPO-34 and its Catalytic Performance in MTO Reaction**

*F. Kalantar Kohdami, J. Towfighi Daryan\*, H. Nemati Arbatani*

*Department of Chemical Engineering, Tarbiat Modares University, Tehran, Iran*

### **Abstract**

*The effect of different crystallization temperatures on the crystallinity, morphology, surface area and catalytic performance of SAPO-34 has been investigated. SAPO-34 catalysts were successfully synthesized using the conventional hydrothermal method. The prepared samples were characterized by XRD, SEM, BET and FTIR techniques. The catalytic performance of the synthesized catalysts was tested in MTO reaction at 410°C and WHSV of 6.5 h<sup>-1</sup>. Temperature of crystallization was found to be the significant parameter for controlling crystallinity and purity, particle size, morphology, surface area and content of hydroxyl groups of the product. The sample prepared at 463 K and 24h possessed the best crystallinity with the smallest crystal size. In the methanol conversion to olefins over SAPO-34 catalysts, this sample showed highest yield of light olefins (88% wt).*

**Keywords:** *MTO Reaction, SAPO-34, Crystallization Temperature, Light Olefins*

### **1. Introduction**

Light olefins such as ethylene and propylene are important raw materials in petrochemical industry and polyolefins production [1]. Conventionally, the lower olefins are produced from crude oil via several processes such as thermal cracking and catalytic cracking. At the same time, the continuous increase in the price of crude oil, the resource limitations in fossil fuels, and the expected reduction in the oil production, make finding another feed instead of crude oil for producing light olefins necessary [2]. Also, the demand for ethylene and propylene, which is predicted to grow faster than its supply, has caused an increased interest in

finding new processes for the production of light olefins [3]. Naphtha steam cracking is a major process for the production of light olefins. The large amount of energy consumption in this process, low yields of light olefins and the carbon dioxide emissions increase the production cost of the light olefins [4]. Methanol to olefin (MTO) process produces light olefins from natural gas or coal via methanol, and has attracted much more attention as an alternative process in recent years. Simple and cheap process and non-petroleum sources as feed were the main reasons for many efforts to develop the process [5]. This reaction is catalyzed by zeolite molecular sieves and the main products of MTO are ethylene and propylene.

---

\* Corresponding author: towfighi@modares.ac.ir

Silicoaluminophosphate molecular sieves (SAPO) are an important class of molecular sieves, which may possess Brønsted acidic sites with the substitution of Si into the neutral framework of  $\text{AlPO}_4$ -n [6]. Aluminophosphate ( $\text{AlPO}_4$ ) molecular sieves' framework is electrically neutral without ion exchange capability [7]. SAPO-34, with the framework of zeolite CHA topology, has eight-ring channels with a pore diameter of 0.38 nm and is much more proper due to the moderate acid strength, relatively small pore diameter, and hydrothermal stability in the MTO process [8,9]. Also, SAPO-34 is the most desirable known catalyst for MTO conversion to date due to the high selectivity of about 80–90% to light olefins ( $\text{C}_2$ – $\text{C}_4$ ) at complete conversion of methanol [10].

Because of similar synthesis conditions, other SAPOs such as SAPO-5 with AFI structure are formed simultaneously as impurity in the synthesis of SAPO-34 molecular sieve process [11]. The structure, physicochemical properties and their applications vary. So, optimal conditions should be used for selective-phase production. SAPO-5 has hexagonal structure twisted in a one-dimensional cylindrical 12-ring framework and SAPO-34 has cubic crystals with 6-ring framework [12]. Recent researches have focused on production of small and pure zeolite and zeolite-like particles with narrow particle size distribution due to considerable increase in their catalytic and separation performances [13-15]. The type of template, silicon and aluminium source, acid concentration, aging time, agitation during crystallization, temperature and time of crystallization were

found to be the significant parameters for controlling crystallinity and purity, particle size and morphology, surface area and acidity of the product. In general, it was found that the crystallinity and size of SAPO-34 were affected dramatically by the temperature, time and mixing condition of crystallization reaction [16].

The influence of synthesis conditions on the physicochemical properties of SAPO-34 as reported in [13,17] was analyzed without relation to the catalytic properties, and in the published data [10,18-20] on the SAPO-34 catalytic activity in the reaction of methanol conversion to lower olefins, make it impossible to correctly assess the effect of synthesis conditions on the properties of the samples, since the catalysts were prepared in various conditions from different groups of precursors.

The aim of the present study was to investigate the synthesis of fine and uniform crystalline particles of SAPO-34 and establish a relation between the temperature of crystallization with particle size and crystallinity of the prepared samples and their catalytic performance in MTO reaction to obtain a suitable catalyst for MTO reaction.

## **2. Experimental**

### **2-1. Catalyst preparation**

Nine SAPO-34 samples were synthesized hydrothermally using different temperatures of crystallization based on the molar compositions of  $1\text{Al}_2\text{O}_3$ :  $1\text{P}_2\text{O}_5$ :  $0.4\text{SiO}_2$ :  $0.5\text{TEAOH}$ :  $1.5\text{MOR}$ :  $70\text{H}_2\text{O}$ , which are presented in Table 1. The source of Al, P and Si were Aluminum isopropoxide (AIP, Merck), phosphoric acid (85% wt  $\text{H}_3\text{PO}_4$ ,

Merck), Silicic acid ( $\text{SiO}_2$ , Merck) respectively. Tetraethyl ammonium hydroxide (20 %wt aqueous solution of TEAOH, Merck) and morpholine (Merck) were used as the organic templates. The synthesis gel was prepared by slowly mixing aluminum isopropoxide to a solution containing phosphoric acid and deionized water with continuous stirring, then silicic acid was added drop wise to the above solution, followed by addition of templates. The obtained gel was aged at room temperature for 8 h with agitation. Agitation could be an appropriate method for increasing the crystallinity. After the aging period the gel was transferred into a 100 mL Teflon-lined stainless steel autoclave. The crystallization process was performed in situ agitation at an adjusted temperature for a fixed period. The synthesized material was recovered by centrifugation, washed six times, and then dried at 383 K for 10 h. The final product was calcinated at 823 K for 5 h.

### **2-2. Characterization**

Phase purity and crystallinity of final product were first verified by X-ray diffraction. The X-ray diffraction (XRD) patterns of catalysts were recorded on a powder X-ray diffractometer (Bruker D8) by using CuK $\alpha$  radiation ( $\lambda = 1.54 \text{ \AA}$ ) operating at 40 kV and 30 mA with a Ni filter in the range of  $2\theta = 5^\circ - 80^\circ$ . The crystal size and morphology was analyzed by scanning electron microscopy (SEM) using Philips XL30 microscopes, operating at 20 kV. Diffuse reflectance FTIR was conducted using a Bruker Tensor-27 spectrophotometer. The FTIR experiments of in-situ heat-treated samples were performed on pure powder of

samples without KBr under Nitrogenflow. IR spectra of the samples in the region of the framework stretching vibrations ( $450-4000 \text{ cm}^{-1}$ ) were measured. The strong and weak acid species of the catalyst were identified and the temperature at which strong acid site absorption bands appeared was determined. The surface areas (BET) and pore volume of calcined samples were determined from isotherm data of nitrogen adsorption-desorption using Micromeritics ASAP-2010 analyzer.

### **2-3. Catalyst performance**

Methanol conversion to olefins was tested under atmospheric pressure and at the temperature of  $410^\circ\text{C}$ . The 1g calcined SAPO-34 catalyst and 2.5 g silicon carbide (as an inert) was packed in the center of stainless steel reactor (internal diameter: 6mm, Length: 8cm) and heated by a tubular furnace. The catalysts were pretreated with 150 ml/min flow of  $\text{N}_2$  at  $550^\circ\text{C}$  for 1 hour then temperature was decreased to reaction temperature ( $410^\circ\text{C}$ ). The liquid mixture of methanol in water (30 wt%) with a weight hourly space velocity (WHSV) of  $6.5 \text{ h}^{-1}$ , was fed by a syringe pump into the reactor. The gas products were analyzed by using a Hewlett-Packard 5890 gas chromatograph equipped with a flame ionization detector and a capillary column to separate the  $\text{C}_1\text{-C}_4$  hydrocarbons. The schematic diagram of the experimental setup used for the MTO process in this study is presented in Fig.1. The conversion of methanol was determined from the outlet liquid sample as the percentage of methanol consumed in the MTO reaction using fractional distillation of outlet liquid.

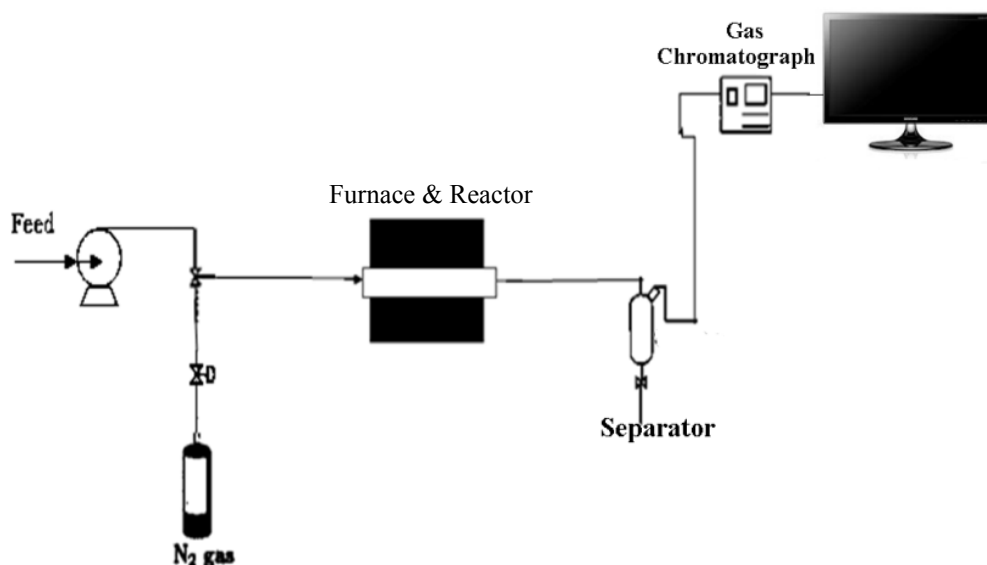


**Figure 1.** Experimental setup used for MTO reaction.

### 3. Results & Discussion

#### 3-1. XRD characterization

The X-ray diffraction pattern of synthesized catalysts prepared by different temperature of crystallization is shown in Fig.2. In order to detect the presence of phase impurity, the obtained patterns were compared with reference pattern [21]. As shown in the figure, the synthesized samples S-1 and S-2 show typical diffraction patterns corresponding to CHA-structure of SAPO-34 at  $2\theta = 9.6, 12.9, 16.0, 20.9, 24.9, 25.9, 30.05, \text{ and } 31.0$  indicating high degree of crystallinity and fewer defects of the samples. The obtained high intensity peaks proved suitable crystallinity of the synthesized samples. In the S-3 sample a small amount of SAPO-5 was detected as impure phase ( $2\theta = 7.5, 21.1$ ) coexisting in the final product of SAPO-34. Depending on the different crystallization temperature used for the synthesis, the degree of crystallinity of the investigated samples varied. According to Table 1 the crystallinity and phase purity increase with increasing

synthesis temperature, from  $170^\circ\text{C}$  up to  $190^\circ\text{C}$  and then decrease. It is due to existence of high value of amorphous phase at  $170^\circ\text{C}$  and  $210^\circ\text{C}$  and also existence of SAPO-5 as impurity at  $210^\circ\text{C}$ . The crystallinity was calculated by dividing the total area of crystalline peaks by the total area under the diffraction curve (crystalline plus amorphous peaks) and, among all samples obtained, the one with the strongest intensities was assigned as the reference with 100% crystallinity, relative crystallinity is presented in Table 1. According to XRD results, Sample S-2 possesses the highest crystallinity.

$$\% \text{crystallinity} = \frac{\sum_{i=1}^3 I_{i,\text{sample}}}{\sum_{i=1}^3 I_{i,\text{reference}}} \times 100 \quad (1)$$

#### 3-2. SEM Characterization

The SEM image of synthesized samples is presented in Fig.3. As shown, S-1 and S-2 samples had cubic like particles with different sizes while for the S-3 a small

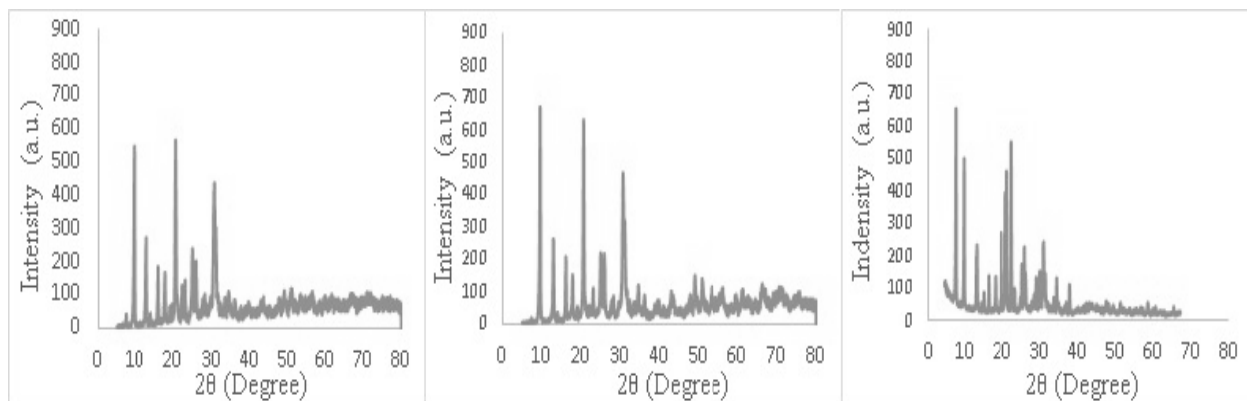


**Figure 2.** XRD pattern of synthesized SAPO-34 with different crystallization temperature.

amount of hexagonal-like particles was present that indicated a small part of SAPO-5 at temperature of 210°C. This is in good agreement with the obtained results from XRD patterns. The average size distribution is presented in Table 1. The S-2 sample had the smallest average particle size. It indicates that crystal size initially decreased and then increased with rise in temperature of crystallization.

### 3-3. Infrared Spectral Analysis (FTIR)

Infrared spectra of the samples in the framework vibration frequency region are shown in Fig.4. The FTIR spectroscopy indicates that the framework characteristic vibration peaks of SAPO-34 are similar to those reported in the literature [22]. Framework vibrations are observed at 490, 530, 640, 720 and 1100  $\text{cm}^{-1}$  that are characteristically similar to those of chabazite. Bending around 1100  $\text{cm}^{-1}$  corresponds to the asymmetric stretch of O-P-O and stretching at 710  $\text{cm}^{-1}$  implies a symmetric stretch of O-P-O; 640  $\text{cm}^{-1}$  indicates the bend of double 6-ring.

Furthermore, 530  $\text{cm}^{-1}$  and 490  $\text{cm}^{-1}$  ascribes the bend of  $(\text{Si,Al})\text{O}_4$  and  $\text{SiO}_4$ , respectively. The band at ca. 1650  $\text{cm}^{-1}$  is assigned to the bonding vibrational mode of the interlayer water molecules [10,17,23]. The last two bands, i.e. 1650, 3450 were attributed to hydroxyl groups of POH, SiOH, and AlOH. In fact, these peaks indicate the adsorption properties of SAPO-34 are due to the presence of acidic sites. There were two hydroxyl stretching vibration bands at 3600 and 3625  $\text{cm}^{-1}$ , which were assigned to Si-OH-Al groups. These hydroxyl groups are the active sites for acid catalyzed reactions. It can be seen that the S2 sample indicates higher concentration of strong acidic hydroxyl groups and S3 sample indicates the lowest concentration of these groups. These results have very good agreement with the results of XRD analysis, and indicate that relative crystallinity and phase purity of final product influences the concentration of strong acidic hydroxyl groups dramatically. In fact, the increase of crystallinity and phase purity in samples increases Si-OH-Al groups.

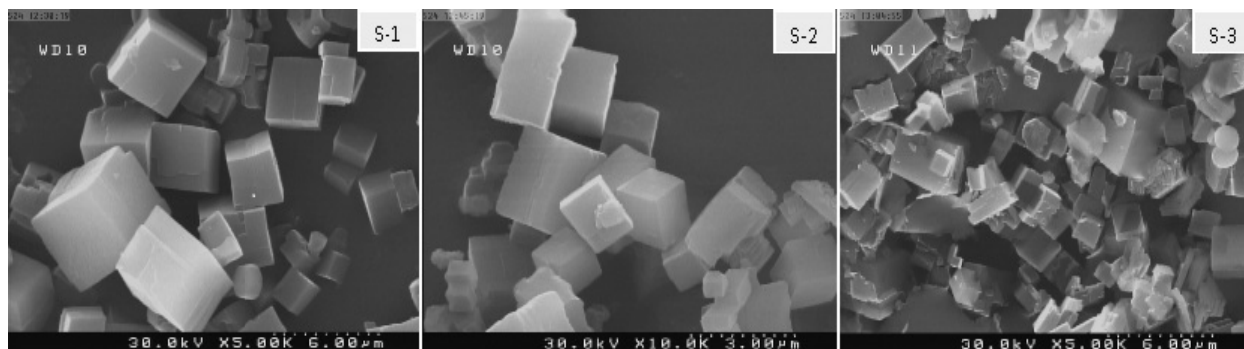


Figure 3. SEM images of calcined samples, S-1, S-2, S-3.

Table 1. Crystallization condition, physical properties and textural data of samples.

| Sample | Product phase  | Temperature (K) | Time (h) | Degree of relative crystallinity (%) | Crystal size distribution ( $\mu\text{m}$ ) | Surface area ( $\text{m}^2/\text{g}$ ) | Pore volume ( $\text{cm}^3/\text{g}$ ) |
|--------|----------------|-----------------|----------|--------------------------------------|---|--|--|
| S-1    | SAPO-34        | 443             | 24       | 88                                   | 1 - 2.75                                    | 500.6459                               | 0.259                                  |
| S-2    | SAPO-34        | 463             | 100      | 0.9 - 2                              | 507.2962                                    | 0.272                                  |  |
| S-3    | Impure SAPO-34 | 483             | 24       | 76                                   | 0.8 - 2.4                                   | 353.9675                               | 0.185                                  |

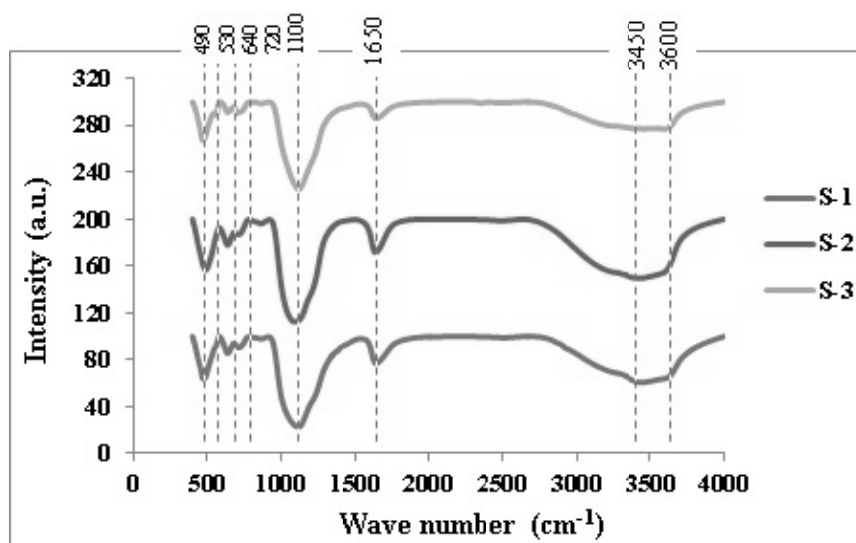


Figure 4. Absorption FTIR spectra of SAPO-34 samples.

### 3-4. Surface area (BET)

The BET surface area and pore volume of samples measured by nitrogen adsorption-desorption experiment are given in Table 1. Based on XRD and SEM results that were discussed earlier, S2 sample had the highest crystallinity and smallest particle size

distribution and, as is seen from Table 1 this sample has the highest surface area. These results showed that decrease of crystallinity and increase of particle size led to decrease of specific surface area. It is worth mentioning that the SAPO-34 exhibits a higher surface area value than SAPO-5 and

as is observed, S3 sample with SAPO-5 impurity exhibits smallest surface area among the other pure SAPO-34 samples. The difference in surface area may be due to variation in channel dimensions. In fact, surface area increased by increasing crystallization temperature up to 463 K and then dramatically decreased.

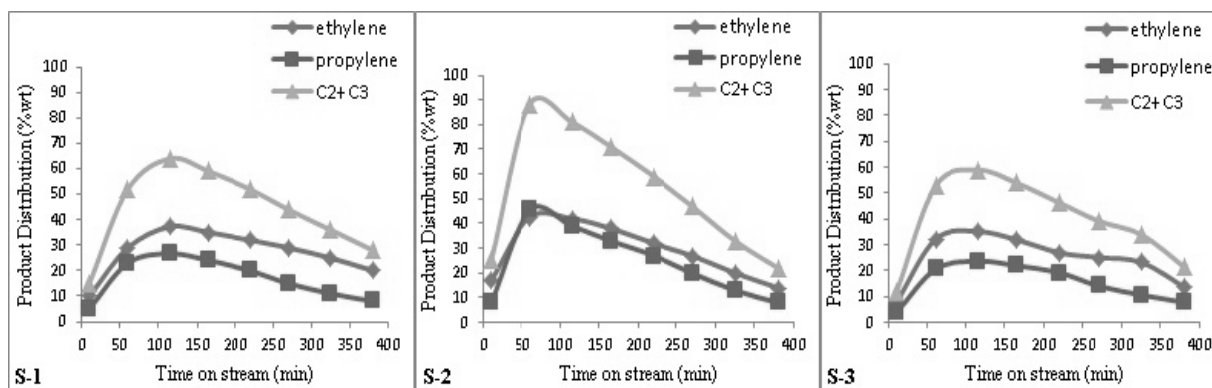
### **3-5. Catalytic performance in MTO reaction**

Catalytic performances of SAPO-34 catalysts synthesized by different crystallization temperatures for methanol to olefins (MTO) reaction were tested at 410°C and WHSV of 6.5 h<sup>-1</sup>. The product distributions of the catalysts with reaction time on the stream (TOS) are shown in Fig.5. Methanol conversion, the maximum yield of ethylene, propylene and light olefins for synthesized samples are shown in Table 2. It was observed that all catalysts obtained over 95% conversion of methanol. All of the prepared samples have the same trend in the total light olefins, but the distribution of products and the maximum yield of light olefins varied significantly. As shown in Table 2, the maximum yield of ethylene is more than propylene for S1 and S3 catalysts. In the MTO process, methanol is dehydrated to DME and the obtained mixture consisting of methanol, DME and water, which are in equilibrium, is converted to light olefins over an acidic catalyst. The rate of formation of ethylene and propylene increased with time and at first, light olefins production achieved the maximum. Then production of light olefins started decreasing [10]. For all catalysts, deactivation is evidenced by the

decline in olefin production, together with the appearance of the intermediate DME, and subsequent decrease of methanol conversion. At first, sample 1 showed low activity, thereafter the production of ethylene and propylene gradually increased with TOS and achieved their maximum values, TOS between 100 and 150 min. Then production of light olefins started decreasing. Sample 2, for TOS between 10 and 20 min showed low activity. There after, production of ethylene and propylene increased, ethylene production is high value at TOS between 50 and 110 and propylene production is maximum value at TOS=50 min. This catalyst showed very good performance in light olefins production (88%wt). In addition, this catalyst indicated smaller particle size distribution and higher relative crystallinity, which, as explained earlier, can improve their catalyst activity. It was observed that the S3 catalyst, in comparison with others, did not achieve a noticeable performance (low olefins yield). The particle size and relative crystallinity of this catalyst were larger and lower than the others, respectively. By increasing the particle size, diffusion resistance will be increased and, therefore, the reactants cannot easily reach the center of the catalyst. As a result, the methanol conversion and yield of light olefins will be decreased [18]. In addition, the maximum product selectivity for these samples decreases in order of S-2>S-1>S-3 which agrees well with intensity of Si-OH-Al bond of these samples in FTIR analysis.

**Table 2.** Methanol conversion and products yield of synthesized catalysts.

| Sample | MeOH Conversion (%) | Light Olefins yield(%wt)      |                               | C <sub>2</sub> =- C <sub>3</sub> =(%wt) |
|--------|---------------------|-------------------------------|-------------------------------|---|
|        |                     | C <sub>2</sub> H <sub>4</sub> | C <sub>3</sub> H <sub>6</sub> |   |
| S-1    | 98                  | 37.3                          | 26.7                          | 64                                      |
| S-2    | 100                 | 42.5                          | 45.5                          | 88                                      |
| S-3    | 96                  | 34                            | 25                            | 59                                      |

**Figure 5.** Products distribution with TOS over synthesized catalysts at 410°C, WHSV of 6.5 h<sup>-1</sup>.

#### 4. Conclusions

SAPO-34 catalysts were synthesized in three different synthesis temperatures under hydrothermal conditions and the effect of crystallization temperature was investigated in this research. The qualification of the product was tested for the response factors as crystallinity, phase purity, the shape, size and surface area of crystalline product. As a result, there is a temperature range below which little reaction occurs and above which zeolite structures and/or template materials are degraded and, at the appropriate range of temperature, temperature has a positive influence on the crystal formation. The results showed that formation of SAPO-5 impurity is enhanced by increasing the crystallization temperature from 463 K up to 483 K. With increasing temperature up to 463 K, the crystallinity of the crystal increased

and the formation of smaller crystals is observed. When temperature exceeds the upper value of the appropriate range (>190°C), the impurity phase such as SAPO-5 co-crystallizes with the main phase. The S-2 sample showed the best qualified product according to the crystallinity which was prepared at 463 K for 24 h. Most of the obtained particles were found to be cubic but for S-3, an amount of hexagonal particles was obtained. The least particle sizes could be achieved at 463 K. Also, recorded FTIR spectra illustrated characteristic vibrational stretches of SAPO-34. The results of MTO reaction tests showed that the crystallinity and particle size distributions are more affected by activity of catalysts. The S-2 sample showed highest yield of light olefins (88% wt).

## References

- [1] Chen, N.Y. and Garwood, W.E., "Industrial application of shape-selective catalysis", *Catal. Rev. Sci. Eng.*, 28, 185 (1986).
- [2] Khadzhiev, S.N., Kolesnichenko, N.V., and Ezhova, N.N., "Manufacturing of lower olefins from natural gas through methanol and its derivatives (review)", *Petro. Chem.*, 48 (5), 325 (2008).
- [3] Li, J., Qi, Y., Liu, Zh., Liu, G., and Zhang, D., "Co-reaction of ethene and methylation agents over SAPO-34 and ZSM-2", *Catal. Lett.*, 121, 303 (2008).
- [4] Park, J. and seo, G., "IR study on methanol-to-olefin reaction over zeolites with different pore structures and acidities", *App. Catal., A: General*, 356, 180 (2009).
- [5] Lee, K.Y., Chae, H.J., Jeong, S.Y. and Seo, G., "Effect of crystallite size of SAPO-34 catalysts on their induction period and deactivation in methanol-to-olefin reactions", *App. Catal. A: General*, 369, 60 (2009).
- [6] Davis, M.E., "Ordered porous materials for emerging applications", *Nature*, 417, 813 (2002).
- [7] Askari, S. and Halladj, R., "Ultrasonic pretreatment for hydrothermal synthesis of SAPO-34 nanocrystals", *Ultraso. Sonochem.*, 19 (3), 554 (2012).
- [8] Vora, B., Chen, J., Bozzano, A., Glover, B., and Barger, P., "Various routes to methane utilization SAPO-34 catalysis offers the best option", *Catal. Today*, 141, 77 (2009).
- [9] Chae, H.J., Song, Y.H., Jeong, K.E., Kim, C.U., and Jeong, S.Y., "Physicochemical Characteristics of ZSM-5/SAPO-34 Composite Catalyst for MTO Reaction", *J. Phys. Chem. Solids.*, 71, 600 (2010).
- [10] Izadbakhsh, A., Farhadi, F., Khorasheh, F., Sahebdelfar, S., Asadi, M., and Yan, Z.F., "Key parameters in hydrothermal synthesis and characterization of low silicon content SAPO-34 molecular sieve", *Microporous and Mesoporous Mater.*, 126, 1 (2009).
- [11] Dargahi, M., Kazemian, H., Soltanieh, M., Hosseinpour, M., and Rohani, S., "High temperature synthesis of SAPO-34: Applying an L9 Taguchi orthogonal design to investigate the effects of experimental parameters", *Powder Technol.*, 217, 223 (2012).
- [12] Weyda, H. and Lechert, H., "The crystallization of silicoaluminophosphates with the structure-type SAPO-5", *Zeolites*, 10 (4), 251 (1990).
- [13] Heyden, H.V., Mintova, S., and Bein, T., "Nanosized SAPO-34 Synthesized from Colloidal Solutions", *Chem. Mater.*, 20 (9), 2956 (2008).
- [14] Hirota, Y., Murata, K., Tanaka, S., Nishiyama, N., Egashira, Y., and Ueyama, K., "Dry gel conversion synthesis of SAPO-34 Nanocrystals", *Mater. Chem. Phys.*, 123 (2), 507 (2010).
- [15] Tosheva, L. and Valtchev, V.P., "Nanozeolites: Synthesis, Crystallization Mechanism, and Applications", *Chem. Mater.*, 17 (10), 2494 (2005).
- [16] Emrani, P., Fatemi, Sh., and Ashraf Talesh, S., "Effect of Synthesis Parameters on Phase Purity, Crystallinity and Particle Size of SAPO-34", *Iran. J. Chem. Chem. Eng.*, 30 (4), 29 (2011).
- [17] Tan, J., Liu, Z., Bao, X., Liu, X., Han, X., He, C., and Zhai, R., "Crystallization and Si incorporation mechanisms of SAPO-3", *Microporous Mesoporous Mater.*, 53, 97 (2002).
- [18] Nishiyama, N., Kawaguchi, M., Hirota, Y., Van, D., Egashira, Y., and Ueyama, K., "Size control of SAPO-34 crystals and their catalyst lifetime in the methanol to olefin reaction", *App. Catal. A: General*, 362, 193 (2009).
- [19] Salmasi, M., Fatemi, S., and Hashemi, S.J.,

- "MTO reaction over SAPO-34 catalysts synthesized by combination of TEAOH and morpholine templates and different silica sources", *ScientiaIranica*, 19 (6), 1632 (2012).
- [20] Álvaro-Muñoz, T., Márquez-Álvarez, C., and Sastre, E., "Use of different templates on SAPO-34 synthesis: Effect on the acidity and catalytic activity in the MTO reaction", *Catal. Today*, 179, 27 (2012).
- [21] Lok, B.M., Messina, C.A., Patton, R.L., Gajek, R.T., Cannan, T.R., and Flanigen, E.M., U.S. Pat. 4440871 (1984).
- [22] Schnabel, K.H., Fricke, R., Girnus, I., Jahn, E., Löffler, E., Parlitz, B., and Peuker, C., "Catalytic and infrared spectroscopic investigations of the molecular sieve types SAPO-34 and SAPO-1", *J. Chem. Soc., Faraday Trans*, 87 (21), 3569 (1991).
- [23] Aghamohammadi, S., Haghghi, M., and Karimipour, S., "A comparative synthesis and physicochemical characterizations of Ni/Al<sub>2</sub>O<sub>3</sub>-MgO nanocatalyst via sequential impregnation and sol-gel methods used for CO<sub>2</sub> reforming of methane", *J. Nanosci. Nanotechnol.*, 13 (7), 4872 (2013).